A NUMERICAL CREEP ANALYSIS ON THE INTERACTION OF TWIN PARALLEL EDGE CRACKS IN FINITE WIDTH PLATE UNDER TENSION

by

Marko D. KATINIC[a], Drazan V. KOZAK[b*], Mirko N. PAVISIC[c] and Pejo I. KONJATIC[b]

[a] Petrokemija d.d., Kutina, Croatia
[b] Mechanical Engineering Faculty J. J. University of Osijek, Slavonski Brod, Croatia
[c] Faculty of Mechanical Engineering, University of Belgrade, Serbia

Original scientific paper
DOI: 10.2298/TSCI130212181K

In many practical situations, high-temperature structures and components contain more than one crack. An interaction of such multiple cracks has significant influence on the service life of structures and components. In this paper, the interaction of two identical parallel edge cracks in a finite plate subjected to the remote tension is numerically analyzed. The results show that interaction effect of multiple cracks at creep regime is obviously greater than at linear elastic regime. The intensity of creep crack interaction increases with increasing creep exponent m. The crack intensity and the crack interaction limit at creep regime depend on crack distance ratio d/a, crack width ratio a/W and creep exponent m.

Key words: *creep, twin cracks, interaction, C* integral*

Introduction

With the increasing demand for reduced CO_2 emissions, the higher operating temperature and design stresses have been adopted in petrochemical and chemical plants and power generation systems to improve the efficiency in energy conversion [1]. This increases the risk of structure failure under creep conditions because the existence of crack-like defects below detection limit cannot be excluded.

In many practical situations, high-temeprature structures and components contain more than one crack. The interaction of multiple cracks changes the stress field around the crack tip and hence changes the crack growth rate. A good understanding of the crack interaction is therefore essential for integrity assessment of the cracked components.

There are several fitness-for-service codes, such as ASME Section XI [2], API579 [3], BS7910 [4], R6 [5] and GB/T 19624 [6], that treat multiple cracks as a single crack if distance between them satisfies a prescribed criteria. However, it should be noted that the multiple crack combination rules are designed to enable safe rather than particularly realistic assessment. This raises the question of whether these rules are in some cases uncertain or too conservative. This especially applies to the case when the structural damage is caused by the phenomenon of creep.

* Corresponding author, e-mail: dkozak@sfsb.hr

Structure integrity assessment can be done using different fracture mechanics parameters depending on actual fracture mechanisms. The stress intensity factor (SIF) [7] is applied in the linear elastic fracture mechanics. In the elastic-plastic fracture mechanics, as parameters are used *J*-integral and crack tip opening displacement (CTOD) [7], which take into account the influence of plastic deformation. For the structure operating at creep regime, the rate dependent parameter *C**-integral [7] is generally used in crack assessment.

Most previous studies have focused on investigation of single cracks and analysis of the interaction of multiple cracks under linear-elastic and elastic-plastic fracture mechanics conditions [8-17]. There are only a few studies that have focused on multiple cracks interaction under creep regime [18-20]. These studies analyze the interaction between twin through wall cracks [19-20] or between twin semi-elliptical surface cracks [18] in finite width plate under tension. Cracks were either in parallel or in coplanar relative position. When twin coplanar cracks are close enough, the stress field around the crack tip will be magnified and hence accelerates the crack growth rate. In contrast to the interaction of coplanar cracks, the stress field around the crack tips of twin parallel overlaped interactive cracks will be decreased due to the shielding effect. For a given crack geometry and position, more pronounced interaction is observed under creep condition compared to that under the linear-elastic range. Also, multiple crack interaction is greater for larger values of the creep exponent *m*.

Very little attention has been paid on the interaction of multiple edge cracks in parallel position. There are only a few studies that have analised twin parallel edge cracks in tension loaded finite width plate under linear-elastic conditions [21-23]. The crack interaction of these cracks is reduced as the distance between cracks increases, thus resulting in linearly decrease of stress shielding effect before converge at certain value. Distance between cracks where the cracks stop interact is called crack interaction limit.

In this study, numerical simulations of interaction were carried out to investigate the effect of crack distance ratio, crack width ratio and creep exponent *m* on interaction intensity and on the determination of crack interaction limit under creep conditions. The finite element (FE) analysis were conducted to evaluate *C**-integral of interacting twin parallel edge cracks in finite width plate under tension.

Finite element analysis

Generally, power law constitutive relationship is appropriate for modeling the stress-strain response under secondary steady state creep. Elastic-secondary creep constitutive relation is as follows:

$$\dot{\varepsilon} = \dot{\sigma}/E + A\sigma^m \tag{1}$$

where $\dot{\varepsilon}$ denotes the uniaxial strain rate, $\dot{\sigma}$ is the uniaxial stress rate, E is Young's modulus. A and m are the steady state creep coefficient and exponent, respectively. The creep fracture parameter *C**-integral under steady-state creep condition is defined as follows:

$$C^* = \int_\Gamma \left[\dot{W} dy - T_i \left(\frac{\partial \dot{u}_i}{\partial x} \right) ds \right] \tag{2}$$

where the notation Γ is used to denote the integral path around the crack tip in anticlockwise direction. T_i is the outward traction vectors on ds, $\dot{u}_i$ is the displacement rate vector

components, x and y are coordinates in a rectangular coordinate system, and ds is the increment on the contour path Γ. Strain energy rate density $\dot{W}$ is given by

$$\dot{W} = \int_0^{\dot{\varepsilon}_{ij}^c} \sigma_{ij} d\dot{\varepsilon}_{ij}^c \tag{3}$$

where σ_{ij} and $\dot{\varepsilon}_{ij}^c$ denote the stress and creep strain rate tensors, respectively.

Using the concept of interaction factor in linear-elastic fracture analysis, one can define the interaction factor for double cracks under creep condition as follows [19-20]:

$$\gamma_c = \sqrt{\frac{C_D^*}{C_S^*}} \tag{4}$$

where γ_c is the creep interaction factor defined as the square root of ratio of C^* integral for double edge cracks to C^*integral for a single edge crack in a finite width plate subjected to the identical remote tension.

Figure 1 depicts twin parallel edge cracks in plate under remote tension σ, with relevant dimensions, considered in the present work. The size of plate considered herein was $H/W = 5$. To reduce the work-load in construction of FE model H and W were fixed. Crack width ratio a/W and crack distance ratio d/a were varied in the following ranges: $0.05 \le a/W \le 0.5$ and $0.5 \le d/a \le 3.0$.

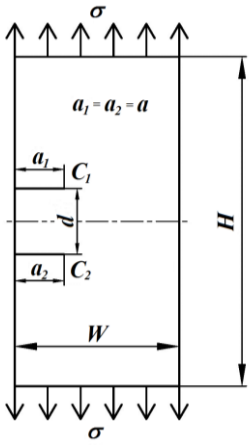

Figure 1 Twin parallel edge cracks in plate under tension

Elastic-secondary creep analysis of the FE model for this case were performed using the general-purpose FE program ABAQUS [24]. It is assumed that the material of the plate is homogeneous and isotropic. In this study mechanical properties of low alloy Cr-Mo steel were used. The material constants of elastic-secondary creep constitutive relation employed in FE analysis are listed in Table 1 [18]. Thus a total of 240 numerical calculation were performed in present work.

Although there is a plane of symmetry, the 2D model of the plate was done completely. Therefore, the seam crack is included in this model. The crack front is chosen to be equivalent to the crack tip. The direction of virtual crack extension at the crack tip is specified by the virtual crack extension direction.

A small geometry change continuum FE model was employed. To avoid problems associated with incompressibility, eight node reduced integration elements for two-dimensional, plain-strain problems (CPE8R) were used. The total meshes varied in different models, but the same number of elements in mesh was used for the crack tip in all cases considered herein. The elements of innermost ring at the crack tip are degenerated into triangles. The three nodes along one side of the eight-node element are defined so that they share the same geometrical place. Each of the three collapsed nodes can be displaced independently. Fig 2. shows the typical FE mesh for a/W = 0.50 and d/a = 1.0. The mesh at the crack tip zone was extremely refined (as shown in Fig. 2b). Five different integral paths around the crack tip were selected during the analysis and the average value of calculated C^*-integral was used at all creep fracture analysis.

Table 1 Material constants used in FE analysis [18]

E / MPa	ν	A / MPa^{-m}h^{-1}	m
200000	0.3	5.0 x 10^{-12}	3
158000	0.3	1.3375 x 10^{-16}	5
144000	0.3	1.9 x 10^{-19}	7
140100	0.3	1.462 x 10^{-24}	9

The domain integral method was used to evaluate C^*-integral in ABAQUS. The method is quite robust in the sense that accurate contour integral estimates are usually obtained even with quite coarse meshes. The method is robust because the integral is taken over a domain of elements surrounding the crack and because errors in local solution parameters have less effect on the evaluated quantity of C^*-integral [24].

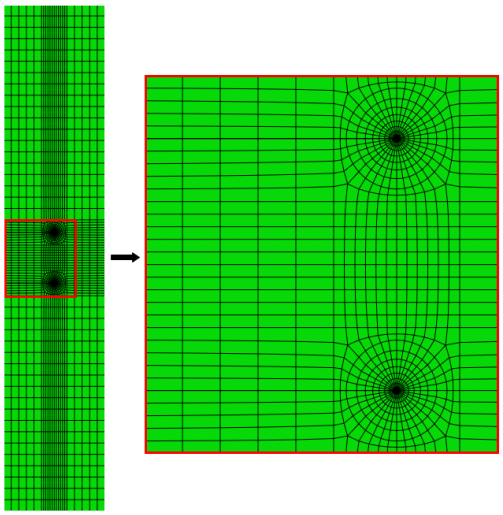

Figure 2 Typical FE mesh for a/W = 0.50 and d/a = 1.0

Initially the edge crack is stress free. The tension load was first applied instantaneously to the FE model using an elastic calculation at time t = 0. The crack tip stress field is, thus, initially characterized by linear elastic fracture mechanics. The load was then held constant and subsequent time-dependent creep calculations were performed. For time-dependent creep calculations, a combined implicit and explicit method was selected within ABAQUS for numerical efficiency. With the load held constant, subsequent creep defor-

mation causes a relaxation of the crack-tip stresses until a steady-state stress distribution is reached. This stress state is characterized by path-independent integral C^* defined by Eq. (2).

To gain confidence in the present FE analysis, the results of FE elastic stress intensity factor (SIF) solutions for single edge crack are compared with well-known solutions [25] in Fig. 3, indicating small differences. The results are given using the dimensionless shape factor F.

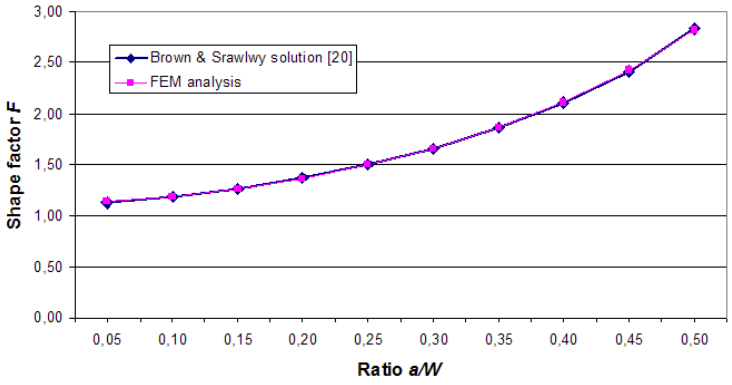

Figure 3 Comparison of shape factor *F* obtained using reference literature [25] and using FEM

Also, Table 3 compares the FE steady-state C^* values with those estimated from GE/EPRI solutions [26] for selected values a/W = 0.25 and 0.50. The results are given using the dimensionless function $h_1(a/W,m)$. As expectedly, a good agreement was obtained, which provides us confidence on the FE modeling of twin edge cracks interaction analysis.

Table 2 Comparison of dimensionless function h_1 (a/W, m) obtained using FEM and literature [26]

a/W	$h_1(a/W, m)$ GE/EPRI	$h_1(a/W, m)$ FEM	*Difference, %*
$A = 5\text{x}10^{-12}$ and $m = 3$			
0.50	2,02	1,99	1,49
0.25	5,20	5,14	1,15
$A = 1.3375 \text{ x } 10^{-16}$ and $m = 5$			
0.50	1,22	1,20	1,64
0.25	4,54	4,48	1,32
$A = 1.9 \text{ x } 10^{-19}$ and $m = 7$			
0.50	0,754	0,736	2,39
0.25	3,87	3,83	1,03

Results and Discussion

Fig. 4 shows the variation of the ratio of the interaction factors in creep and linear elastic conditions γ_c/γ_{SIF} depending on the crack distance ratio d/a for different crack width ratios a/W and selected creep exponent m = 3. The crack interaction in creep condition is more pronounced than in linear-elastic condition. For example, for the case a/W = 0.45 and d/a = 1.0 the interaction factor in creep condition γ_c is about 24 % higher than the interaction factor in linear-elastic condition γ_{SIF}. However, the discrepancy between the interaction factors γ_c and γ_{SIF} decreases with the decreasing crack width ratio a/W as shown in Fig. 4. For ratios $a/W \leq 0.20$ the corresponding ratio γ_c/γ_{SIF} is slightly higher than 1 and is approximately constant for all the considered range of the ratio d/a.

Trend variation the ratio γ_c/γ_{SIF} for different values of the creep exponents m is similar for all the cases considered herein. However, the ratio γ_c/γ_{SIF} for selected ratios a/W and d/a is higher for higher exponents m. Fig. 5 shows the variation of the ratio γ_c/γ_{SIF} depending on creep exponent m for all considered crack distance ratio d/a and selected crack width ratio $a/W = 0.45$. In range of crack interaction the crack interaction in creep condition for higher values of creep exponents m is more pronounced than in linear-elastic condition. This conclusion applies to other considered ratios a/W.

Figure 6 shows the influence of crack distance ratio d/a on the interaction factor γ_c for different crack width ratios a/W and selected creep exponent $m = 3$. The interaction factor γ_c is the highest for $a/W = 0.50$ at $d/a \approx 0.90$. However, the crack interaction for $a/W = 0.50$ exists in a narrow range of d/a. Namely, the interaction factor γ_c for $a/W = 0.50$ starts to converge toward the value of 1 at $d/a \approx 2.5$, which represents the crack interaction limit in creep condition. For $a/W = 0.45$ the crack interaction factor γ_c has maximum value at $d/a \approx 1.30$. This maximum is lower than the maximum for $a/W = 0.50$. However, the crack interaction for $a/W = 0.45$ exists in the wider range of d/a than in the case of $a/W = 0.50$. The interaction factor γ_c for $a/W = 0.45$ converges toward the value of 1 at $d/a = 3.0$. From all other graphs shown in Fig. 6, it can be concluded that the corresponding maximum of the interaction factor γ_c is lower for lower values of a/W and, in this case, its location is shifted to higher values of d/a. In general, the crack interaction exists in the wider range of ratios d/a in the case of lower values of a/W. From the corresponding graphs, it can be supposed that the crack interaction limits for $a/W \leq 0.40$ are reached at values $d/a > 3$. The crack interaction limits for lower values of a/W are at higher values of d/a. To determine the interaction limits for different a/W, it would be necessary to carry out additional numerical calculations for $d/a > 3$. It is beyond the scope of this paper.

In some cases, for different ratios a/W the crack interaction factor γ_c is lower than 1. Range of the ratios d/a in which the factor γ_c is lower than 1 is wider for lower ratios a/W. Thus, for example, in the case of the ratios $a/W = 0.15$, 0.10 and 0.05 the factor γ_c is less than 1 in the entire observed range of the ratio d/a. On the other hand, for example, in the case of the ratio $a/W = 0.35$ the factor γ_c is less than 1 only in range of the ratio $d/a < 1$.

Figure 7 shows the influence of crack distance ratio d/a on the interaction factor γ_c for different crack width ratios a/W and selected creep exponent $m = 5$. There is a great similarity between the corresponding graphs shown in Fig. 6 and 7. The entire discussion of the results in Fig. 6 can be applied to the results in Fig. 7. However, one can see the difference in interaction intensity between the case in Fig. 6 and the case in Fig. 7. For example, the crack interaction factor γ_c for ratio $a/W = 0.45$ and $d/a = 1.0$ is significantly higher in the case when $m = 5$. Fig. 8 and 9 show the variation of the interaction factor γ_c depending on the ratio d/a for creep exponents $m = 7$ and $m = 9$, respectively. Since there is a great similarity between the corresponding graphs shown in the Fig. 6, 7, 8 and 9 it is clear that the same discussion and conclusions can be applied in all the studied cases.

From Fig. 6, 7, 8 and 9 it is clear that interaction effect is more pronounced for higher values of exponent m. For example, the crack interaction factor γ_c for ratio $a/W = 0.45$ and $d/a = 1.0$ is the highest in the case when $m = 9$ and is the lowest in the case when $m = 3$. The influence of creep exponent m on interaction factor γ_c for the selected ratio $a/W = 0.45$ is shown in Fig. 10. Generally, this conclusion holds valid for other considered values of the ratio a/W. However, the discrepancy between the interaction factors γ_c for different values of the exponent m decreases with the decreasing crack width ratio a/W. This is evident when comparing Fig. 10 and 11.

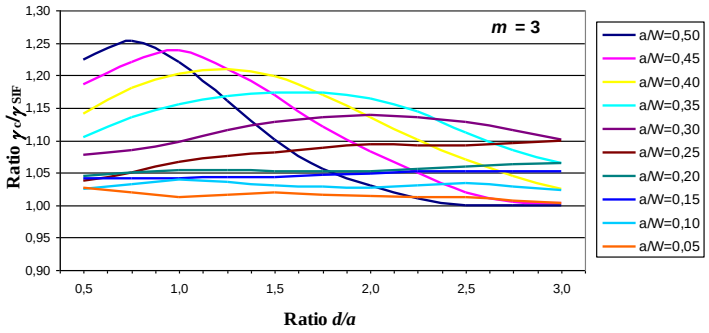

Figure 4 Ratio γ_c/γ_{SIF} vs. ratio d/a for $m = 3$

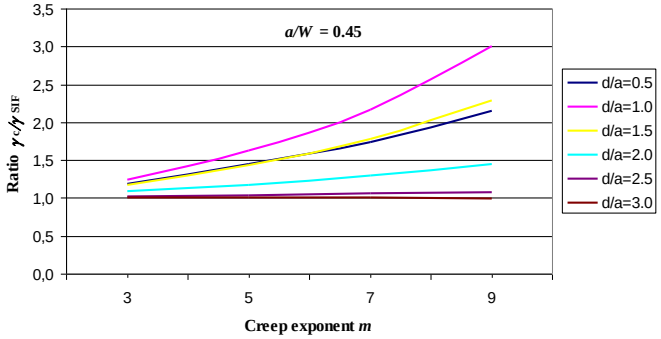

Figure 5 Ratio γ_c/γ_{SIF} vs. exponent m for $a/W = 0.45$

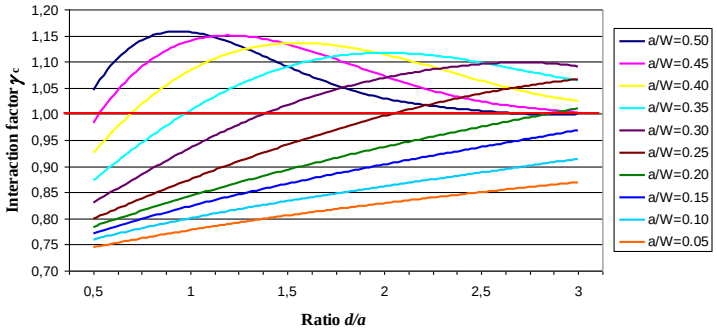

Figure 6 Interaction factor γ_c vs. ratio d/a for different ratios a/W and $m = 3$

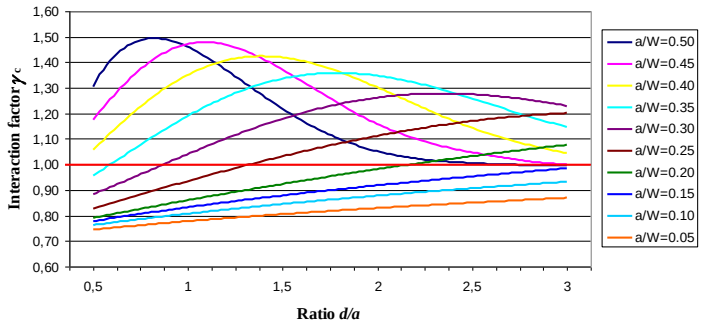

Figure 7 Interaction factor γ_c vs. ratio d/a for different ratios a/W and $m = 5$

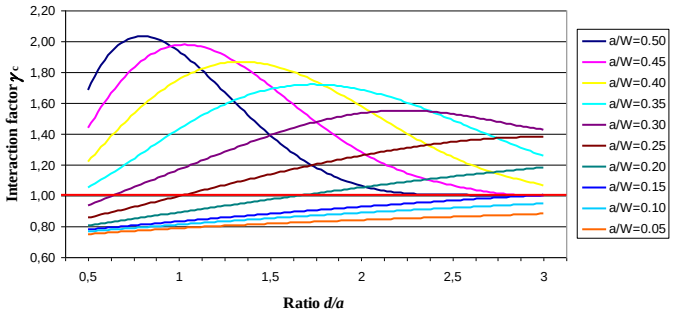

Figure 8 Interaction factor γ_c vs. ratio *d/a* for different ratios *a/W* and *m* = 7

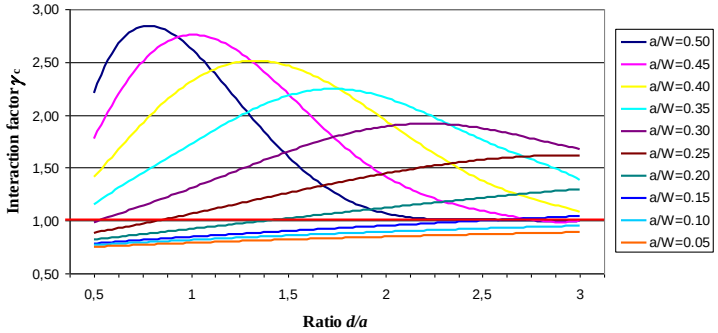

Figure 9 Interaction factor γ_c vs. ratio *d/a* for different ratios *a/W* and *m* = 9

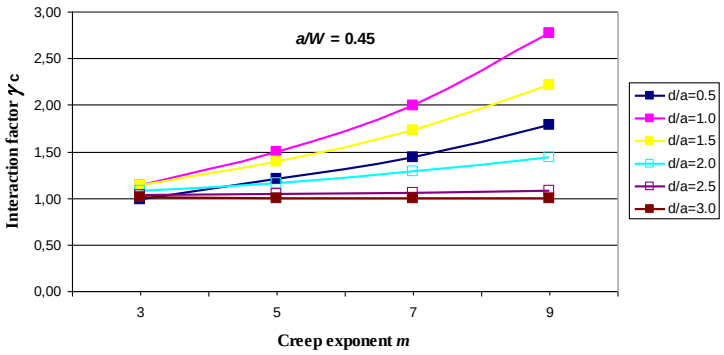

Figure 10 Interaction factor γ_c vs. exponent *m* for different ratios *d/a* and ratio *a/W* = 0.45

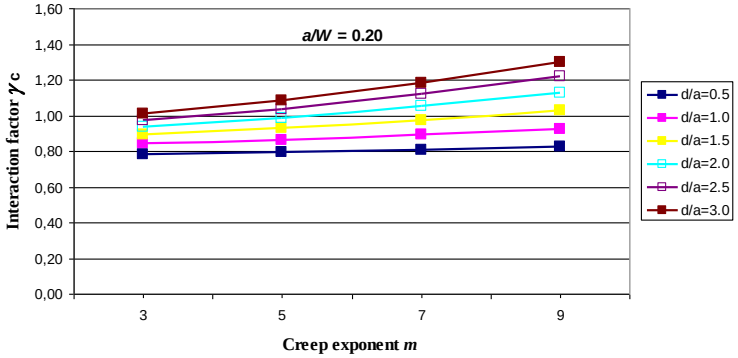

Figure 11 Interaction factor γ_c vs. exponent *m* for different ratios *d/a* and ratio *a/W* = 0.20

Conclusions

Interaction effect on *C** parametar of twin parallel edge cracks in plate under tension has been analyzed on the basis of the comprehensive FE creep calculations. The main conclusions are listed as follows:

- The interaction effect of multiple cracks at creep regime is obviously greater than at linear elastic regime, which should be taken into account when assessing the integrity of high-temperature component with crack-like defects.
- The interaction effect of multiple cracks at creep regime is influenced by crack distance ratio *d/a*, crack width ratio *a/W* and creep exponent *m*.
- The present FE calculations have proven the abilities to define the crack interaction limit in creep regime, which also depends on values of crack distance ratio *d/a*, crack width ratio *a/W* and creep exponent *m*.

References

[1] X. Liu, F. Z. Xuan, J. Si, S. T. Tu, Expert system for remaining life prediction of defected components under fatigue and creep-fatigue loadings, Expert syst. applic., 34, pp. 222-230, 2008.
[2] ASME, Boiler and Pressure Vessel Code Section XI, New York, 2007.
[3] American Petroleum Institute, API 579-1/ASME FFS-1, Fitness-for-service, Section 9, 2007.
[4] Guidance on Methods of Assessing the Acceptability of Flaws in Metallic Structures, Brtish Standard Institutions, London, UK, BS7910, 2005.
[5] Assessment of the Integrity of Structures Containing Defects, British Energy Generation Ltd., Gloucester, Revision 4, R6, 2006.
[6] Safety Assessment for In-Service Pressure Vessels Containing Defects, Chinese Standards, Beijing, GB/T19624, 2004.
[7] S. Damnjanovic, A. Sedmak, H. A. Anyiam, N. Trisovic, Lj. Milovic, C* Integral Evaluation by Using EPRI Procedure Structural Integrity and Life, Vol. 2, No 1-2, 2002, pp. 51-54.
[8] R. Sethurman, G. Reddy, I. T. Ilango, Finite element based evalution of stress intensity factors for interactive semi-elliptic surface cracks, Int. J. Press. Vess. Piping, 80, 2003, 12, pp. 843-5t
[9] M. Manjgo, B. Medjo, Lj. Milovic, M. Rakin, Z. Burzic, A. Sedmak, Analysis of welded tensile plates with a surface notch in the weld metal and heat affected zone, Eng. Fract. Mech., 77, 15, pp. 2958-2970, 2010.
[10] D. Kozak, N. Gubeljak, P. Konjatic, J. Sertic, Yield load solutions of heterogeneous welded joints, Int. J. Press. Vess. Piping, 86, pp. 807-812, 2009.
[11] P. Konjatic, D. Kozak, N. Gubeljak, The Influence of The Weld Width on Fracture Behaviour of The Heterogeneous Welded Joint, Key Engineering Materials, 488-489, pp. 367-370, 2012.
[12] N. Gubeljak, J. Predan, D. Kozak, Leak-Before-Break Analysis of a Pressurizer - Estimation of the Elastic-Plastic Semi-Elliptical Through-Wall Crack Opening Displacement, Structural Integrity and Life, Vol. 12, No. 1, 2012, pp. 31-34
[13] I. Camagic, N. Vasic, Z. Vasic, Z. Burzic, A. Sedmak, Compatibility of fracture mechanics parameters and fatigue crack growth parameters in welded joint behaviour evaluation, Technical Gazette, Vol. 20, 2, pp. 205-211, 2013.
[14] Yu. G. Matvienko Development of Models and Criteria of Notch Fracture Mechanics, Structural Integrity and Life, Vol. 11, No. 1, 2011, pp. 3-7
[15] P. Agatonović, Proposal for the improved design of reliable failure assessment diagrams for components with surface crack, Structural Integrity and Life, Vol. 13, No. 2, 2013, pp. 99-108
[16] A. Carpinteri, R. Brighenti, S. Vantadori, A numerical analysis on the interaction of twin coplanar flaws, Eng. Fract. Mech., 71, 2004, 1-6, pp. 485-499.
[17] W. A. Moussa, R. Bell, C. L. Tan, Interaction of two parallel non-complanar identical surface cracks under tension and bending, Int. J. Press. Vess. Piping, 76, 1999, 3, pp. 135-145
[18] S. Jun, X. Fu-Zhen, T. Shan-Tong, A numerical creep analysis on the interaction of twin semi-elliptical cracks, Int. J. Press. Vess. Piping, 85, 2008, 7, pp. 459-467
[19] X. Fu-Zhen, S. Jun, T. Shan-Tong, Evalution of *C** integral for interacting cracks in plates under tension, Eng. Fract. Mech. 76, 2009, 14, pp. 2192-2201

[20] X. Fu-Zhen, S. Jun, T. Shan-Tong, Rules for assessment of interacting cracks under creep conditions, Journal of Press. Vess. Techn., 132, 011405-1-6, 2010.
[21] R. Daud, M. A. Rojan, A. K. Ariffin, S. Abdullah, Elastic crack interaction limit of two interacting edge cracks in finite body, ICADME 2012, Panag, Pulan Pinang, Malesia
[22] R. Daud, A. K. Ariffin, S. Abdullah, Al Emran Ismail, Interacting cracks analysis using finite element method, Applied Fracture Mechanics, 27-28 February 2012, Penang, Malaysia. DOI:20.5772/54358
[23] Z. D. Jiang, A. Zeghloul, G. Bezine, J. Petit, Stress intensity factor of parallel cracks in a finite with sheet, Eng. Fract. Mech. 35, 1990, 6, pp. 1073-1079
[24] ABAQUS User's Manual. Version 6.10 Dassault Systems Simulia Corp., Providence, RI, USA
[25] W. F. Brown Jr., J. E. Srawlwy, Plane strain crack toughness testing of high strength metallic materials, ASTM STP 410 , 1966, 12
[26] C. F. Shih, A. Needleman, Fully plastic crack problems, Part 1: Solutions by a penalty method, Journal of Applied Mechanics, Vol. 51, 1984, 1, pp. 48-56

Paper submitted: February 12, 2013
Paper revised: June 16, 2013
Paper accepted: June 25, 2013